Laser Monitoring of Non-Newtonian Liquids During Dip Coating

Alexandre F. Michels
Centro de Ciências Exatas e Tecnologia, Universidade de Caxias do Sul, CEP 95070-560, Caxias do Sul, RS, Brazil

Pedro Lovato and Flavio Horowitz
Instituto de Física - Universidade Federal do Rio Grande do Sul (UFRGS), Campus do Vale, CP15051, 91501-970, Porto Alegre, RS, Brazil

DOI 10.1002/aic.11834
Published online September 16, 2009 in Wiley InterScience (www.interscience.wiley.com).

Dip coated films, widely used in the coating industry, are usually measured by capacitive methods with micrometric precision. In this work, interferometric determination of thickness evolution in real time, for the first time to our best knowledge, is applied to volatile non-Newtonian liquids with several viscosities and distinct dip withdrawing speeds. Thickness evolution during the process depends on time as predicted by a power law model. Comparison with measured results (uncertainty of ± 0.007 μm) showed very good agreement after initial steps of the process. © 2009 American Institute of Chemical Engineers *AIChE J,* 55: 3052–3055, 2009
Keywords: coating flows, fluid mechanics, optics, process control

Introduction

Among wet bench films production processes, dip coating is widely used especially for fabricating coatings on nonplanar or long-dimension objects.[1] Although dip coating requires simple equipment and small resources, its dynamics of film deposition may become complex, with different stages during the process.

In this sense, extensive theoretical studies have been devoted to describe Newtonian fluid behavior under dip coating,[2,3] as well as several empirical observations.[4–7] However, in these experimental studies, film thicknesses are traditionally measured by capacitive techniques with large uncertainties (±2 μm), which are also influenced by other parameters, such as substrate or belt thickness variations.[5]

More recently, accurate optical techniques have been used to spatially measure film profiles by an interferometric technique,[8,9] or for temporally monitoring physical thickness evolution during the process.[10] Comparison between experimental physical thickness evolution and theoretical results, within a precision much higher than that of the traditional capacitive method in the physical thickness determination (uncertainty of ±0.007 μm), are reported for Newtonian mineral oils, with constant refractive index during dip coating.[10]

For more complex liquids, with significant refractive index variation during the process, polarimetric and interferometric techniques were combined (double optical monitoring) to determine variable refractive index and variable physical thickness values, simultaneously and in real time.[11]

Application of the double-optical monitoring method to a sol–gel sulfated zirconia colloid, with variable refractive index, allowed comparison between experimental physical thickness evolution and theoretical predictions, where in the first stage, dominated by mass loss, the film was shown to be practically unaffected by evaporation and to flow as a Newtonian liquid.[12]

However, in spite of the numerous theoretical and experimental papers about non-Newtonian properties,[13–15] to our best knowledge still there is no experimental study reporting temporal physical thickness evolution of non-Newtonian liquids during the dip coating process that would allow precise tests of existing theories.

Correspondence concerning this article should be addressed to A. F. Michels at alexandrefassinimichels@gmail.com

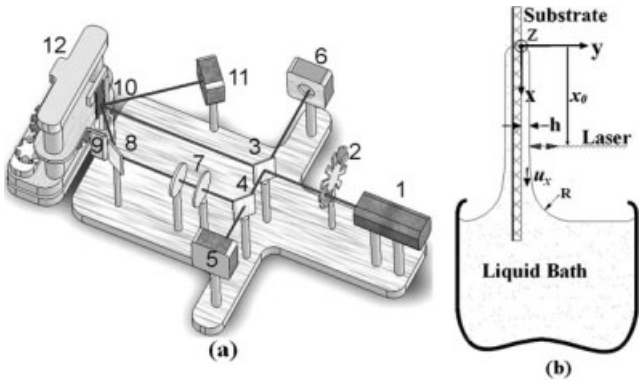

Figure 1. (a) Optical monitor setup, composed of laser beam at λ = 660 nm (1), chopper (2), beam splitters (3, 4), reference detector (5), sample detectors (6, 11), polarizer (7), mirror (8), liquid bath (9), sample (10), and dip coater (12); (b) illustration of the dip coating batch process, where laser probing is shown.

The spot under measurement corresponds to a fixed value in the vertical x-axis.

This is focused in this work, for power-law and volatile liquids (carbopol and carboxymethyl cellulose (CMC)), by use of the double-optical monitoring method, and aiming at a comparison between experimental results and theoretical predictions.

Experimental

Synthesis

Typical mixtures of carbopol-934 (a water-soluble semi-synthetic polymer, in which groups of CH_2COONa substitute OH in cellulose chains, forming esters) and CMC (commercial name for polymers composed of long chains of polyacrylic acid cross-linked with allylsucrose), were considered. According to the Gutfinger and Tallmadge procedure,[13] carbopol and CMC powders were first dissolved in deionized water, in distinct concentrations of 0.20 and 0.50 mol L^{-1}. The powdered form of these polymers was obtained from Chemidex.

The colloidal suspension was prepared by adding powder to deionized water under magnetic stirring, at 500 rpm for 1 h, to achieve a transparent solution, according to the Labanda et al. procedure.[16] Afterward, the colloidal suspension was homogenized by ultra-sound and filtrated using an FTFE membrane (millipore with 5 μm pore size). The resultant transparent suspensions were used to coat clean silicon substrates by the dip coating process.

Optical measurements

Monitoring of the CMC and carbopol (mixture) film deposition properties is obtained by analysis of the reflected signal from a diode laser beam (1), at wavelength l = 660 nm. The double-optical monitoring setup is shown in Figure 1a, more details can be found in Ref. 11.

The sample and the double-optical monitoring system are vibration isolated from the dip coater. To prevent contamination, as well as temperature inhomogeneities, the bath container is routinely kept inside a transparent chamber. In all experiments, the relative humidity and the temperature of the dip coater chamber are controlled (at 90% and 24°C respectively). The measuring spots, produced at low power from the attenuated microwatts laser source, do not affect the temporal pattern of the interference fringes, thus indicating that local heating does not influence film properties.

Systematic errors in optical thicknesses data were excluded by comparison with those obtained by ellipsometry. Systematic errors in refractive index data were eliminated by calibration using oil standards of known refractive indices at 25°C, and by comparison with ex situ Abbe refractometry results at the processing temperature of 24°C.[13]

Refractive index values were obtained during the dip coating process by averaging every 10 successive measurements, at a sampling rate of 1.7 KHz, corresponding to the maximum random error uncertainty shown in Table 1. Also in this table, maximum random error uncertainty in the temporal occurrence of quarterwave optical thickness variations is presented, associated with localization of the extremes in the reflectance temporal curve, whose data was acquired every 0.3 ms.

Theoretical

The extremes in the interference-modulated curve can be written as a function of the film optical thickness (nh) as[17]:

$$nh\cos\phi = M\frac{\lambda}{4}, \tag{1}$$

where n is the film refractive index and h its physical thickness; ϕ is the angle with the interface normal inside the film, λ is the wavelength of light in vacuum, and M is an integer number. In reflection, for a film with a refractive index larger than that of the substrate, Eq. 1 applies to interference minima for M even and to interference maxima for M odd.

Physical thickness evolution of a liquid film on a substrate with infinite length in the dip coating continuous process can be described, under steady-state flow, by a simplified form of the Landau–Levich equation[2,3]:

Table 1. Fitting Values and Physical Properties of the Non-Newtonian Liquids

Non-Newtonian Liquids	Withdrawal Speed, U (mm/s)	Refractive Index, n (liquid film)	Refractive Index, n (gel)	Density, ρ (Kg/m^3)	Final Thickness h_f (μm)	Power Index, s	K (Stokes)
Carbolpol 0.1 mol L^{-1}	12	1.3341 ± 0.0005	1.3360 ± 0.0005	1000 ±1	10.7 ± 0.9	0.79 ± 0.08	0.0055 ± 0.0002
CMC 0.2 mol L^{-1}	12	1.3330 ± 0.0005	1.3342 ± 0.0005	1000 ± 1	27.2 ± 0.2	0.38 ± 0.02	0.12 ± 0.01
CMC 0.5 mol L^{-1}	12	1.3335 ± 0.0005	1.3343 ± 0.0005	1000 ± 1	46.8 ± 0.3	0.28 ± 0.02	0.31 ± 0.03
CMC 0.5 mol L^{-1}	10	1.3335 ± 0.0005	1.3343 ± 0.0005	1000 ± 1	27.3 ± 0.2	0.24 ± 0.02	0.29 ± 0.02
CMC 0.5 mol L^{-1}	7	1.3335 ± 0.0005	1.3343 ± 0.0005	1000 ± 1	24.3 ± 0.4	0.17 ± 0.03	0.30 ± 0.04
CMC 0.5 mol L^{-1}	2	1.3335 ± 0.0005	1.3343 ± 0.0005	1000 ± 1	22.6 ± 0.7	0.14 ± 0.04	0.31 ± 0.07

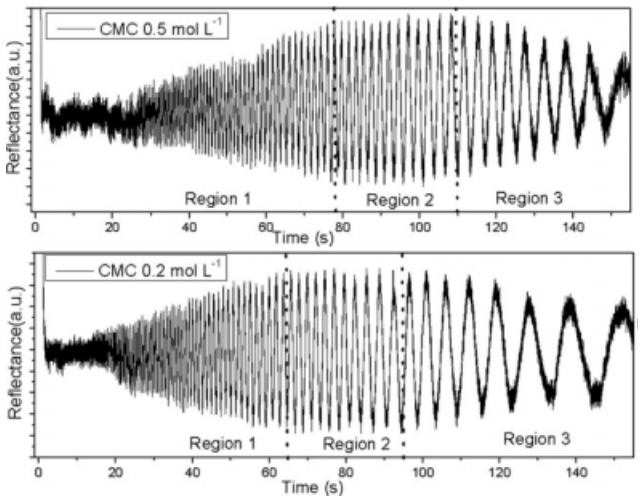

Figure 2. Reflectance temporal evolution for carboxymethyl cellulose (CMC), with two concentrations during the dip coating process.

$$\frac{\sigma}{\rho}\frac{\partial^3 h}{\partial x^3}+\frac{1}{\rho}\frac{\partial \tau_{xy}}{\partial y}+g=0, \tag{2}$$

where ρ is the liquid density, g the gravity force, τ_{xy} is shear stress, and σ is related to surface tension. These tree terms represent the surface tension, the viscous and de gravitational effects, respectively. In a region far away from the static meniscus, the surface tension effect may be neglected and Eq. 2 can be expressed as:

$$\frac{1}{\rho}\frac{\partial \tau_{xy}}{\partial y}+g=0, \tag{3}$$

For non-Newtonian liquids, the shear stress and shear rate do not present a linear relation. For fluids that follow the power-law behavior, the shear stress is related with velocity variation by a power index "s" though the relation:

$$\tau_{xy}=K\left|\frac{\partial v_x}{\partial y}\right|^{s-1}\frac{\partial v_x}{\partial y}; \tag{4}$$

where "K" is the rheological constant. Equation 1, with Eq. 2 and initial conditions:

$$u_x(y=0)=u_0 \tag{5a}$$

$$\left|\left(\frac{\partial u_x}{\partial y}\right)^s\right|_{y=h}=0 \tag{5b}$$

give the physical thickness (h) evolution,

$$h(x,t)=\left(\frac{K}{\rho g}\right)^{\frac{1}{s+1}}\left(\frac{x}{t}\right)^{\frac{s}{s+1}}, \tag{6}$$

where x/t corresponds to the withdrawing speed u for an observer in the laboratory reference system, shown in Figure 1b.

Results and Discussion

By use of the double optical monitoring method,[11] experimental results were obtained for two volatile non-Newtonian liquids (carbopol and CMC) with distinct viscosities, and under several withdrawing speeds.

Figure 2 shows the raw data, as reflectance interferograms, obtained from the temporal evolution of carbopol, with distinct concentrations, where in accordance with Eq. 1 each interval between successive extremes corresponds to an optical thickness variation, nh, of $\lambda/4$.

The interferograms, shown in Figure 2, may be divided into three distinct regions. In the first one, dominated by mass drainage,[12] a continuous increase in reflectance amplitude was observed, due to a reduction of light scattering as the film becomes thinner. After a short period of stability during the second region, a significant reduction of reflectance amplitude is seen in the third region. The film then becomes gradually translucent, and whitish to the naked eye, probably as a result of solvent evaporation.

Furthermore, in Figure 2, the observed decrease in time interval between successive extremes, since refractive index is kept nearly constant by the low evaporation rate at high humidity (as later shown in Figure 3) can be attributed to the temporal decrease of the physical thickness $h(x,t)$. This can be explained from relation (6), which at a constant laser probing position, x, leads to the temporal variation

$$\frac{\partial h}{\partial t}\propto t^{-\left(\frac{2s+1}{s+1}\right)}, \tag{7}$$

whose value decreases with time for $s>0$.

Through these $\lambda/4$ step intervals of nh, and by direct polarimetric measurement of the refractive index, n, in real time, information about physical thickness, h, evolution was achieved during the process, as shown in Figure 3.

In a previous investigation,[12] the beginning of the evaporation mass loss stage was identified through refractive index monitoring. However, this was not possible for the volatile non-Newtonian liquids in this study, due to the small variation of refractive index between the liquid and the jellified film, as shown in Figure 2. Ex situ measurements performed by Abbe refractometry (Table 1) confirmed this small variation.

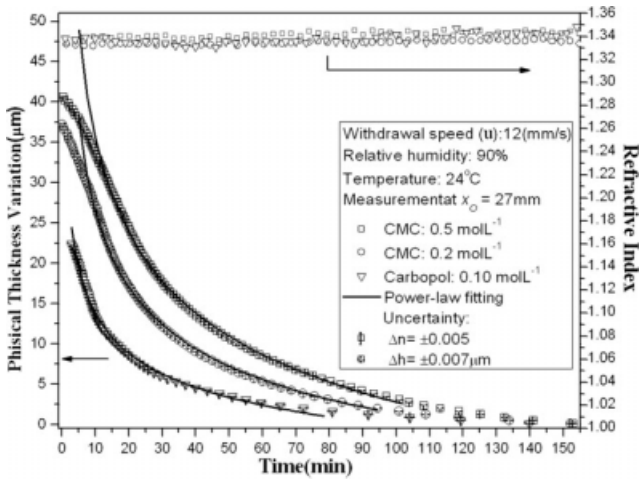

Figure 3. Temporal evolution of physical thickness and refractive index during dip coating of carbopol and carboxymethyl cellulose (CMC) at distinct concentrations.

Although experimental points were obtained at each $\lambda/4$ variation, only data at each λ variation are shown for better visualization. Modeling results are shown in solid curves. Displayed uncertainties are specified at the inset.

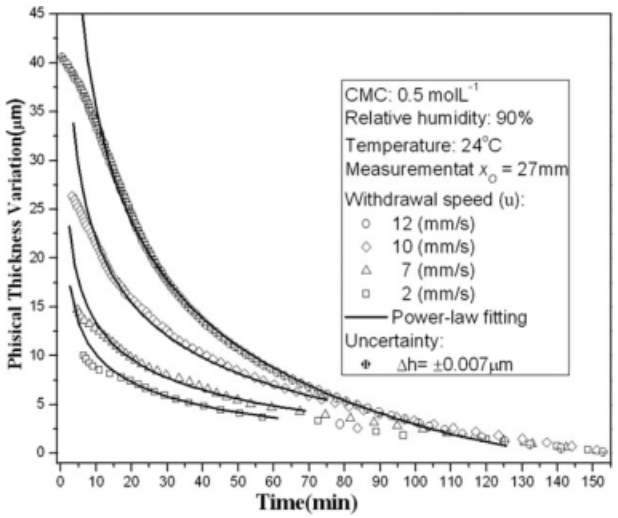

Figure 4. Temporal evolution of physical thickness during dip coating of carboxymethyl cellulose (CMC), at different withdrawal speeds, with process parameters and uncertainties specified at the inset.

Modeling results are shown in solid curves. Although experimental points were obtained at each $\lambda/4$ variation, only data at each λ variation are shown for better visualization.

In Figure 3, we note that as the CMC concentration increases, so does the mass loss in the same time interval. This does not imply in a smaller optical thickness value, which would contradict Eq. 2, since the initial thickness is larger for a higher viscosity.

Similarly, we note in Figure 4 that as the withdrawing speed increases, so does the mass drain in the same time interval. On the other hand, Eq. 2 indicates that a larger film thickness adheres to the substrate for a faster withdrawing speed. These two observations are consistent, since a thicker film allows faster flow in its most external layers.

Now, we focus on the comparison between experimental results and the theoretical power-law predictions shown as solid lines in Figures 3 and 4. The agreement attained, after the very initial moments of the process, indicates that the experimental data, within the uncertainty of ± 7 nm, agree well with the values obtained from are non-Newtonian power-law relation (2).

In Figures 2 and 3, for both CMC concentrations, good agreement is shown between experimental results and theoretical power-law predictions until the beginning of region 3. Later on, possibly the influence of solvent (H_2O) evaporation becomes relevant to film viscosity. In a similar way, increase of withdrawal speed, shown in Figure 4, delays the influence evaporation, thus making possible agreement with model predictions through a longer period.

The theoretical fitting parameters, K and s, are compatible with previous reports by Gutfinger and Tallmadge involving carbopol.[14]

Further characterization and understanding of the process temporal dynamics of non-Newtonian liquids, we believe, might facilitate control and optimization of their film formation temporal parameters for a variety of applications.

Concluding Remarks

First double-optical analysis during batch dip coating of non-Newtonian fluids was presented for carbopol and CMC. Quantitative description of temporal thickness variation was then achieved since the beginning of the process at an acquisition rate of 3.5 KHz.

After the initial few seconds, the experimental data agreed very well with the dependence predicted by the power-law model. This agreement corroborates the validity of the analytical theoretical treatment for power-law fluids, as well as reinforces applicability of the double-optical method—with nanometric precision in physical thickness variation—for quantitative analysis for quantitative analysis of the dip coating process dynamics with complex non-Newtonian liquids.

Acknowledgments

This work was supported by CNPq (Conselho Nacional de Desenvolvimento Científico e Tecnológico), in collaboration with Empresa Brasileira de Compressores (EMBRACO and LNLS) National Synchrotron Light Laboratory, Brazil.

Literature Cited

1. Scriven LE. Physics and applications of dip coating and spin coating. *Mater Res Soc*. 1988;121:717–729.
2. Landau LD, Levich BG. Dragging of a liquid by a moving plate. *Acta Physicochim*. 1942;17:42–54.
3. Levich BG. *Physicochemical Hydrodynamics*. New Jersey: Prentice-Hall, 1962.
4. White DA, Tallmadge JA. Free coating of a Newtonian liquid onto a vertical surface. *Chem Eng Sci*. 1965;20:33–37.
5. Groenveld P. Withdrawal of power law fluid films. *Chem Eng Sci*. 1970;25:33–40.
6. Spiers RP, Suraman CV, Wilkinson WL. Free coating of a Newtonian liquid onto a vertical surface. *Chem Eng Sci*. 1973;29:389–396.
7. Schunk PR, Hurd AJ, Brinker CJ. Free-Meniscus Coating Processes. In: Kistler SF, Schweizer PM, editors. *Liquid Film Coating*. London: Chapman & Hall, 1997: 673–708.
8. Nishida F, McKiernan JM, Dunn B, Zink JI, Brinker CJ, Hurd AJ. In situ fluorescence probing of the chemical changes during sol-gel thin film formation. *J Am Ceram Soc*. 1995;78:1640–1648.
9. Qu D, Rance E, Garoff S. Dip coated films of volatile liquids. *Phys Fluids*. 2002;14:1154–1156.
10. Michels AF, Menegotto T, Horowitz F. Interferometric monitoring of dip coating. *Appl Opt*. 2004;43:820–823.
11. Michels AF, Grieneisen HP, Susin MB, Menegotto T, Horowitz F. Double optical monitoring. *Appl Opt*. 2006;45:1491–1494.
12. Michels AF, Menegotto T, Santilli CV, Horowitz F. Temporal evolution of sulfated zirconia sol-gel during dip coating: analysis of mass drainage with time-varying refractive index. *J Non-Cryst Solids*. 2006;352:5362–5367.
13. Gutfinger C, Tallmadge JA. Films of non-newtonian fluids adhering to flat plates. *AIChE J*. 1965;11:403–413.
14. Spiers RP, Subabaraman CV, Wilkinson WL. Free coating of non-newtonian liquids onto a vertical surface. *Chem Eng Sci*. 1975;30: 379–385.
15. Tallmadge JA. Withdrawal of flat plates from power law fluids. *AIChE J*. 1970;16:925–930.
16. Labanda J, Marco P, Llorens J. Rheological model to predict the thixotropic behaviour of colloidal dispersion. *J Labanda J Llorens, Colloids Surf A*. 2004;249:123–126.
17. Born M, Wolf E. *Principles of Optics*, 6th ed. Cambridge: Cambridge University Press, 1997.

Manuscript received Mar. 24, 2008, and revision received Dec. 31, 2008.